Available online at www.sciencedirect.com
ScienceDirect
Biochimica et Biophysica Acta 1777 (2008) 55–65
Biochimica et Biophysica Acta BBA
www.elsevier.com/locate/bbabio

Energy transfer processes in *Gloeobacter violaceus* PCC 7421 that possesses phycobilisomes with a unique morphology

Makio Yokono [a], Seiji Akimoto [b,*], Kohei Koyama [c], Tohru Tsuchiya [c,d], Mamoru Mimuro [c,d]

[a] *Institute of Low Temperature Science, Hokkaido University, Sapporo 060-0819, Japan*
[b] *Molecular Photoscience Research Center, Kobe University, Kobe 657-8501, Japan*
[c] *Graduate School of Human and Environmental Studies, Kyoto University, Kyoto 606-8501, Japan*
[d] *Department of Technology and Ecology, Hall of Global Environmental Research, Kyoto University, Kyoto 606-8501, Japan*

Received 13 August 2007; received in revised form 1 November 2007; accepted 2 November 2007
Available online 12 November 2007

Abstract

We examined energy transfer dynamics in phycobilisomes (PBSs) of cyanobacteria in relation to the morphology and pigment compositions of PBSs. We used *Gloeobacter violaceus* PCC 7421 and measured time-resolved fluorescence spectra in three types of samples, i.e., intact cells, PBSs, and rod assemblies separated from cores. *Fremyella diplosiphon*, a cyanobacterial species well known for its complementary chromatic adaptation, was used for comparison after growing under red or green light. Spectral data were analyzed by the fluorescence decay-associated spectra with components common in lifetimes with a time resolution of 3 ps/channel and a spectral resolution of 2 nm/channel. This ensured a higher resolution of the energy transfer kinetics than those obtained by global analysis with fewer sampling intervals. We resolved four spectral components in phycoerythrin (PE), three in phycocyanin (PC), two in allophycocyanin, and two in photosystem II. The bundle-like PBSs of *G. violaceus* showed multiple energy transfer pathways; fast (≈10 ps) and slow (≈100 ps and ≈500 ps) pathways were found in rods consisting of PE and PC. Energy transfer time from PE to PC was two times slower in *G. violaceus* than in *F. diplosiphon* grown under green light.

Keywords: Chromatic adaptation; Energy transfer; Phycobilisome; Time-resolved fluorescence; *Gloeobacter violaceus*

1. Introduction

Photosynthetic organisms possess specific antennae that capture light energy and subsequently transfer excitation energy to the reaction centers where primary photochemical reactions take place. Cyanobacteria are the most primordial among oxygenic photosynthetic organisms, and their antenna systems consist of phycobiliproteins that form a supramolecular assembly, the phycobilisome (PBS), located outside of the thylakoid membranes [1–11]. Two types of PBSs are found in cyanobacteria and red algae; the hemidiscoidal form and the hemiellipsoidal form. The hemidiscoidal PBS has been extensively studied [1,12], and the rod and the core structure were found. Phycobiliproteins are classified into three types; phycoerythrin (PE), phycocyanin, (PC) and allophycocyanin (APC). Each phycobiliprotein forms trimers or hexamers with specific linker proteins [11]. Crystal structures of individual phycobiliproteins have been well resolved from many different organisms [5,6,13], however the structures with linkers are still unknown for PE and PC. Optically, PE shows the highest energy level among the three and it contains phycoerythrobilin as chromophores, except for some organisms in which an additional chromophore, phycourobilin, is also present. PC and APC both contain phycocyanobilin as chromophores, and PC has a higher energy level than APC as a result of interaction with protein [5].

The most primordial cyanobacterium, *Gloeobacter violaceus* PCC 7421, which was scraped from the surface of limestone in Switzerland, has a bundle-like PBS that is attached to the cytoplasmic membranes, not to the thylakoid membranes [14–

Abbreviations: APC, allophycocyanin; FDAS, fluorescence decay-associated spectra; PBS, phycobilisome; PC, phycocyanin; PE, phycoerythrin; PS, photosystem; SVD, single value decomposition; TRFS, time-resolved fluorescence spectra

* Corresponding author. Tel./fax: +81 78 803 5705.
E-mail address: akimoto@hawk.kobe-u.ac.jp (S. Akimoto).

0005-2728/$ - see front matter © 2007 Elsevier B.V. All rights reserved.
doi:10.1016/j.bbabio.2007.11.001

16]. *G. violaceus* shows unique properties among cyanobacteria. It lacks thylakoid membranes but has only cell membranes that lack sulfoquinovosyl diacylglycerol [17]. A few genes encoding subunits of photosystem II (PS II) are missing (*psbY*, *psbZ* and *psb27*) [18]. The PBS does not possess a rod-core linker (L_{RC}) CpcG, but contains two new linker proteins, CpeG and CpcJ [16], and the unusual CpcC [19]. The former two have sequences corresponding to proteins with three linker motifs in tandem. It was proved that CpeG functions as a rod linker (L_R) connecting PE and PC, while CpcJ functions as an L_{RC} connecting PC and APC [16,18]. Three rod elements are associated by the CpcJ to form a large rod called the rod assembly (Fig. 1a). These two linkers support a unique bundle-like morphology of PBSs in *G. violaceus* that may cause differences in energy transfer processes and/or kinetics.

Excitation energy transfer processes in PBSs have been examined by steady-state spectroscopy and time-resolved spectroscopy [20–22]. Transfer kinetics or transfer processes have sometimes been discussed in relation to PBS morphology. Furthermore, energy transfer process(es) in sub-components of PBSs, which were isolated from cells or PBSs, were also discussed. For example, Zhang's group estimated the time constant for energy transfer from PC (rod) to APC (core) as 18 ps based on phycobiliprotein crystal structures and time-resolved fluorescence spectra (TRFS) of the rod-core complex [23]. Yamazaki and co-workers focused on the isolated APC-B trimer with a linker polypeptide, and showed that the APC-B trimer contains an energy-sink subunit, the α-subunit of APC-B, to which an energy transfer occurs with a time constant of 140 ps at −196 °C [24].

Energy transfer processes of PBSs have been analyzed by time-resolved fluorescence spectroscopy because a large shift of the fluorescence peaks can be clearly observed. A combination of the fluorescence decay curves and global analysis yielded fluorescence decay-associated spectra (FDAS), which is comparable to decay-associated spectra (DAS) in absorption changes. Time resolution has improved during the last 20 years, however spectral resolution has not necessarily been fully improved. In the present study, we examined energy transfer dynamics in *G. violaceus* by means of picosecond time-resolved fluorescence spectroscopy with an improved spectral resolution. We used three samples prepared from *G. violaceus*, i.e. intact cells, isolated PBSs, and isolated rod assemblies. *Fremyella diplosiphon* shows a complementary chromatic adaptation, and was used as a control. In intact PBSs of *G. violaceus*, a rod assembly contains three rods of PE and PC, and two such rod assemblies may interact with each other (Fig. 1a). On the other hand, when rod assemblies are separated from the core, CpcJ is not associated with rods [16], therefore a rod assembly consists of three rods, and each of the rods is composed of three PE hexamers and three PC hexamers. In PE, chromophores are comprised of phycourobilin in addition to phycoerythrobilin. The APC core consists of three dodecamer units and two hexamer units. The former contains APC, APC-B, core-membrane linker or L_{CM} (ApcE), 18.3 kD protein (ApcD), and L_C (ApcC). On the other hand, *F. diplosiphon* can change the composition of phycobiliproteins in response to light quality [25]; this is known as complementary chromatic adaptation. The cells grown under green light synthesized PE, PC, and APC, and those grown under red light synthesized only PC and APC. Changes in the pigment composition are reflected as changes in the composition of PBS rods, i.e. the PE-PC rods of the green-grown cells or the PC rods in the red-grown cells, and there are three hexamers in total under both growth conditions. As shown in Fig. 1, morphology and pigment contents differ between *G. violaceus* and *F. diplosiphon*, which may cause differences in the energy transfer processes and their kinetics. Here, we examine these points and discuss the transfer processes in relation to the morphology of PBSs.

2. Materials and methods

G. violaceus PCC 7421 was cultured autotrophically in BG-11 medium under fluorescent light (10 μE m^{-2} s^{-1}) at 25 °C [14]. *F. diplosiphon* IAM M-100 was cultured autotrophically in BG-11 medium at 25 °C. Light conditions for the red-grown cells were a combination of red fluorescent light (FL10P, Mitsubishi/Osram) and a four-layer red vinyl chloride filter (AH143, 0.5 mm thickness, Sekisui-seikei, Osaka, Japan). For the green-grown cells, green fluorescent light was used (FL10G, Mitsubishi/Osram) with a green vinyl

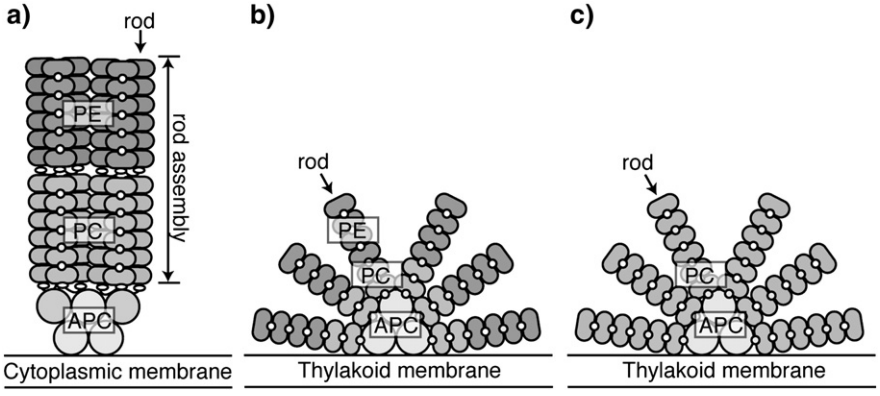

Fig. 1. Models of PBSs in a) *G. violaceus* and b, c) *F. diplosiphon* grown under two light conditions. A rod assembly consists of three rods bundled by a novel linker (CpeG), and it attaches to the core via a novel linker, CpcJ. Schematic model of hemidiscoidal PBS in b) *F. diplosiphon* grown under green light and c) *F. diplosiphon* grown under red light.

chloride filter (TM1600, 0.5 mm thickness, Morino-kako, Saitama, Japan). PBSs were isolated from *G. violaceus*, and rod assemblies were separated from PBSs by methods described by Koyama et al. [16].

Absorption and steady-state fluorescence spectra were recorded using a spectrophotometer (Hitachi 557) and a spectrofluorometer (Hitachi 850), respectively. The spectral sensitivity of the fluorometer was corrected by the radiation profile of the standard lamp (Hitachi, Japan). The second derivative spectra were obtained by the method developed by Savitzky and Golay [26]. TRFS were measured by the time-correlated single-photon counting method at −196 °C [27]. Samples were mixed with the same volume of poly(ethylene glycol) 4000 (30%, w/v) (Wako Pure Chemicals, Japan) to obtain homogeneous ice and were frozen in the dark. The light source was a Ti:sapphire laser and the excitation wavelength was 398 nm, which brought about excitation of phycobiliproteins and/or Chl *a*. An absorption probability of phycobiliproteins is almost proportional to amounts of individual proteins. Spectral data were measured with a 2-nm interval and stored, and TRFS were reconstructed afterwards. FDAS were calculated as follows: fluorescence decay curves were deconvoluted using free-running exponential components with an instrument function. After deconvolution, the time resolution was improved to approximately 3 ps. All the decays were re-analyzed using the same lifetime parameters. The amplitudes of these exponential components as a function of emission wavelength provided FDAS [28]. Spectral decomposition analysis was also performed and similar results were observed (data not shown) [20].

3. Results

3.1. Steady-state absorption and fluorescence spectra

Fig. 2a shows the absorption spectra of intact cells, PBSs, and rod assemblies of *G. violaceus* at room temperature. PE exhibited two peaks at 502 nm and 565 nm with a shoulder at 550 nm in all samples. These peaks originated from phycourobilin (502 nm) and phycoerythrobilin (550 nm and 565 nm). PC showed a peak at 624 nm and APC at 650 nm, and those originated from phycocyanobilin. The absorption spectrum of rod assemblies demonstrated the absence of APC. Chl *a* showed two peaks at 440 nm and 680 nm in the spectrum of intact cells, corresponding to the Soret and Q_y bands, respectively. The absorption spectra of intact cells of *F. diplosiphon* at room temperature are shown in Fig. 2b. The green-grown cells showed a peak of PE at 565 nm, but the 502-nm band was not recognized, indicating the lack of phycourobilin. The red-grown cells showed the peak of PC at 624 nm, but PE peaks were not detected. The APC and Chl *a* peaks were located at 650 nm and 680 nm, respectively.

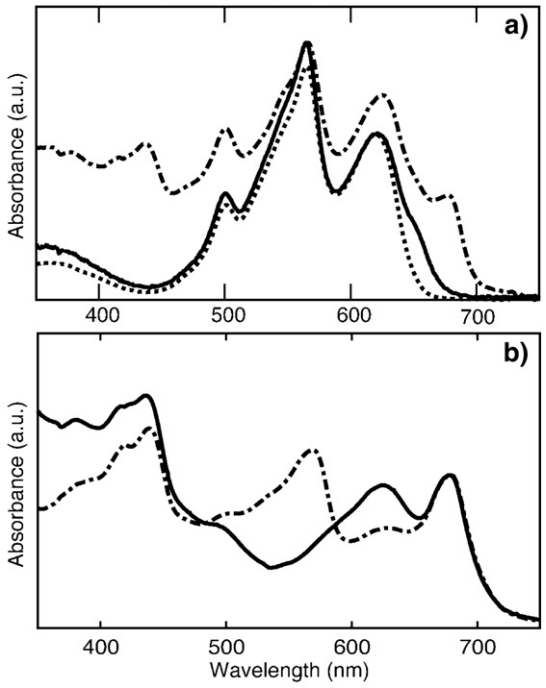

Fig. 2. Absorption spectra of *G. violaceus* and *F. diplosiphon* at room temperature. a) Intact cells (dot-dashed line), PBSs (solid line), and rod assemblies (dotted line) of *G. violaceus*. b) Intact cells of the *F. diplosiphon* grown under green light (dot-dashed line) and under red light (solid line); spectra were normalized at 678 nm.

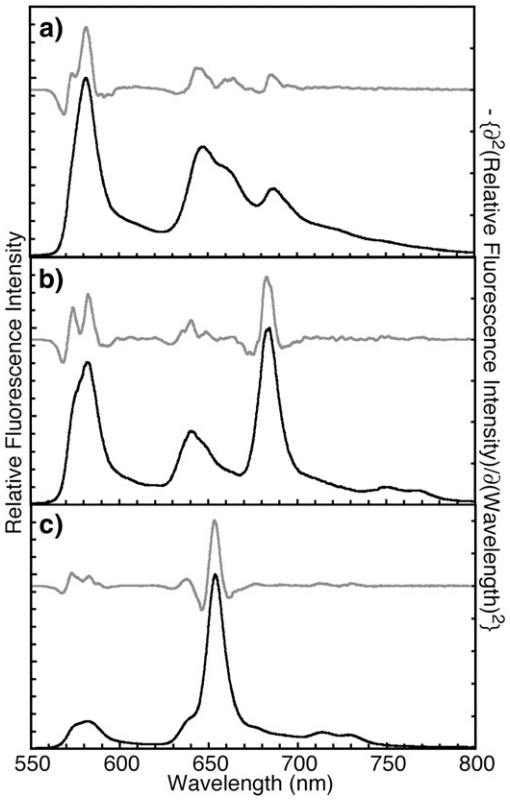

Fig. 3. Fluorescence spectra (black line) and its second derivative spectra (gray line) of a) intact cells, b) PBSs, and c) rod assemblies of *G. violaceus*. Spectra were measured at −196 °C, and spectral sensitivity of the apparatus was numerically corrected. Excitation wavelength was 500 nm.

Fig. 3 shows fluorescence spectra of the three samples of *G. violaceus* at −196 °C upon excitation at 500 nm. In the case of intact cells, four apparent maxima were observed at 582 nm, 647 nm, 660 nm, and 686 nm. Fluorescence bands were clearly resolved by the second derivative spectrum, and shown to be located at 573 nm, 582 nm, 640 nm, 646 nm, 651 nm, 662 nm, 685 nm, and 695 nm; these came from PE, PE, PC, PC, PC, APC, PS II Chl *a*, and PS II Chl *a*, respectively. There was no PS I Chl *a* fluorescence at 720–740 nm, which is consistent with results of previous studies [29,30]. Isolated PBSs showed spectra with a few differences (Fig. 3b); the peak of PE was detected at 573 nm and 582 nm, and PC bands were resolved to

635 nm, 640 nm, and 648 nm. An APC form appeared around 662 nm, and the terminal components of PBSs were resolved to two, i.e. at 682 nm and 684 nm. The presence of plural terminal components was consistent with a report on *Nostoc* sp. [31]. In the long-wavelength region, vibrational bands of APC were detected at 748 nm and 770 nm, where energy differences from the main band were 1250 cm^{-1} and 1630 cm^{-1}, respectively [32]. In the case of rod assemblies, the main emission of PC was located at 652 nm, and due to its high intensity, an emission of PE was apparently low (Fig. 3c). Vibrational bands of PC were localized at 711 nm and 732 nm.

Fluorescence spectra of *F. diplosiphon* intact cells at −196 °C upon excitation at 398 nm are shown in Fig. 4. In the case of the green-grown cells (Fig. 4a), five maxima were observed at 584 nm, 648 nm, 662 nm, 685–695 nm, and 739 nm, and those came from PE, PC, APC, PS II Chl *a* and PS I Chl *a*, respectively. The red-grown cells exhibited only four maxima at 651 nm, 662 nm, 685–695 nm, and 739 nm coming from PC, APC, PS II Chl *a* and PS I Chl *a*, respectively (Fig. 4b).

3.2. Time-resolved fluorescence spectra

Fig. 5 shows reconstructed TRFS of *G. violaceus* at −196 °C represented in contour, with time expressed as a logarithmic scale. The TRFS of intact cells initially showed maxima of PE and PC fluorescence at approximately 560 nm and 630 nm, respectively (Fig. 5a). These peaks showed a red-shift with time; the former shifted to 582 nm with a shoulder at 572 nm, and the latter to 651 nm, reflecting energy transfer among individual phycobiliproteins. These fluorescence signals originated from phycoerythrobilin in PE and phycocyanobilin in PC, respectively. PE contains phycourobilin as a chromophore

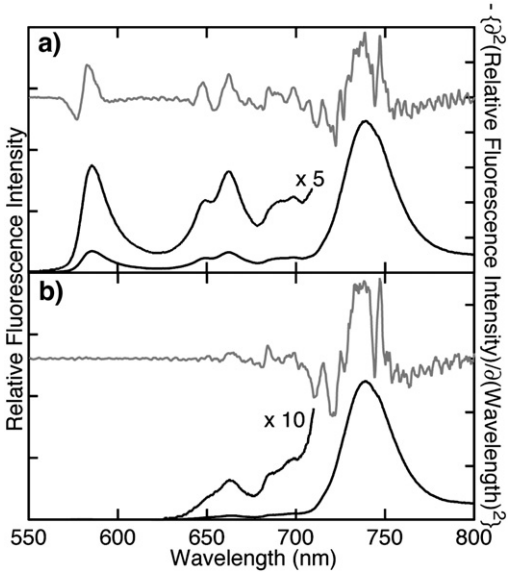

Fig. 4. Fluorescence spectra (black line) and its second derivative spectra (gray line) of intact cells of *F. diplosiphon* grown under a) green light and b) red light. Spectra were measured at −196 °C, and spectral sensitivity of the apparatus was numerically corrected. Excitation wavelength was 398 nm.

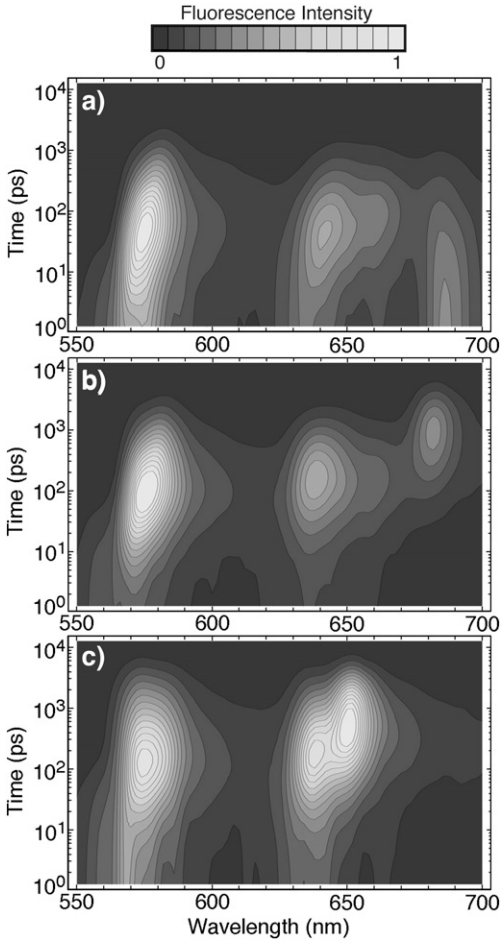

Fig. 5. Time-resolved fluorescence spectra of a) intact cells, b) PBSs, and c) rod assemblies of *G. violaceus* at −196 °C. Fluorescence intensity is expressed as a gradation shown in the upper side of the figure, and black indicates a low intensity. The sampling interval of the original data was 2 nm.

(Fig. 2a), which is expected to exhibit fluorescence at approximately 515 nm originating from the 502-nm absorption band. However, no significant fluorescence peak was observed in this wavelength region for all the samples examined here, even though this region was not shown in the figure. This suggested that energy transfer from phycourobilin was an ultrafast process that was shorter than our time resolution. In the APC spectral region, a peak at 660 nm appeared in 50–100 ps, but fluorescence from the APC terminals was not detected. Instead, Chl *a* fluorescences of PS I and PS II were clearly detected. The fluorescence from PS I Chl *a* arose at approximately 690 nm (Mimuro et al., unpublished) and that from PS II Chl *a* at 684 nm. The blue-shift of the maxima with time reflected that Chl *a* fluorescence at the longer wavelength region (PS I) decayed with a shorter lifetime than that of PS II.

The TRFS of PBSs just after excitation were essentially the same as that of intact cells except for the absence of Chl *a* fluorescences (Fig. 5b). In the time-region of 100 ps, the PC maximum remained around 640 nm, showing a lack of the fast energy pathway from the PC 640-nm form (hereafter, we denote the spectral form by a name of phycobiliprotein and peak

wavelength, e.g. PC_{640}), contrary to the case of intact cells. Associated with decay at 660 nm in the time-region of 200 ps, the APC terminal emitter appeared at 682 nm (APC-B and/or L_{CM}), which indicates the slow energy transfer from APC_{660} to the APC terminal emitter. The maximum of the APC terminals was located at 682 nm, a significantly shorter wavelength than that of Chl *a* in intact cells.

In rod assemblies, PE and PC exhibited fluorescence peaks at the same wavelength as those in intact cells and PBSs at the very beginning (Fig. 5c). However, the PE peak did not shift to 582 nm; the peak remained at 572 nm with a shoulder at 582 nm, showing PE_{572} could not efficiently transfer their energy to PE_{582}. The 651-nm PC emission arose in 400 ps, indicating slow energy transfer to the PC terminal emitter at 651 nm.

Fig. 6 shows TRFS of *F. diplosiphon* intact cells at −196 °C represented in contour. The green-grown cells showed the dynamic red-shift in PE, PC, APC, and PS II Chl *a* regions, and the fluorescence intensities decreased faster than in *G. violaceus* in all wavelength regions (Fig. 6a). In a longer time-region (approximately 200 ps), five peaks remained at 582 nm, 647 nm, 665 nm, 693 nm, and 735 nm; those originated from PE, PC, APC, PS II Chl *a*, and PS I Chl *a*, respectively. The TRFS of the red-grown cells of *F. diplosiphon* were essentially identical to those of the green-grown cells except for the lack of PE fluorescences (Fig. 6b). A new band was observed around 650 nm; this was a feature of the red-grown cells and it might correspond to the red-most form of PC, suggesting the presence of an additional PC hexamer contributing to fast energy transfer within PC. A short-lived component at 615 nm was scarcely observed (see later).

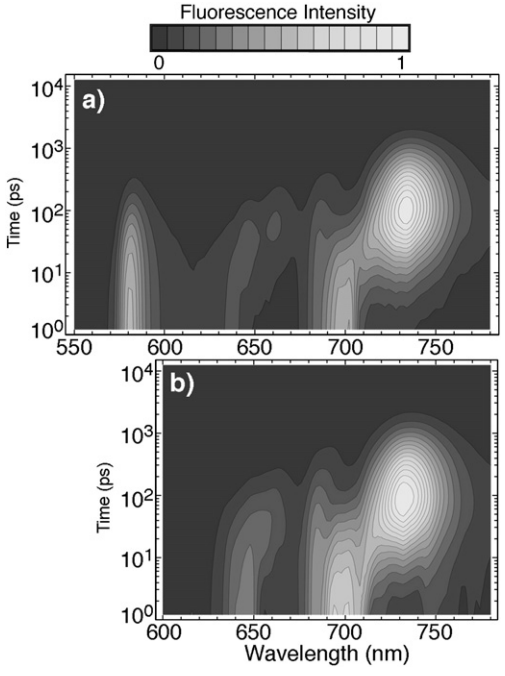

Fig. 6. TRFS of intact cells of *F. diplosiphon* −196 °C grown under a) green light and b) red light. Fluorescence intensity is expressed as a gradation shown in the upper side of the figure, and black indicates a low intensity. The sampling interval of the original data was 2 nm.

4. Analysis based on fluorescence decay-associated spectra

We applied the FDAS method to resolve TRFS into spectral forms of pigments with the same rise and decay profiles (Fig. 7 for *G. violaceus* and Fig. 8 for *F. diplosiphon*). The number of lifetime components was estimated independently by the single value decomposition (SVD) method. In FDAS, negative and positive bands indicate rise and decay kinetics in populations in the excited state, respectively. Coupling of negative and positive bands is a clear indication of energy transfer from the pigments giving the positive band to those giving the negative band. However, in some cases, only a negative band is resolved. One explanation is that an energy donor (D) transfers energy to an acceptor (A_1) with a faster time constant than our time resolution, and subsequent energy migration occurs within the same kinds of acceptors ($D \rightarrow A_1 \rightarrow A_1$). In this case, no clear positive peak of the energy donor (D) would be observed in the shorter wavelength region of a negative band of energy acceptors (A_1). The other explanation is that an energy acceptor (A_1) transfers energy to the next acceptor (A_2) faster than it receives energy from a donor (D) in a sequential energy transfer chain ($D \rightarrow A_1 \rightarrow A_2$). In this case, the latter process ($A_1 \rightarrow A_2$) is resolved as a negative component in fluorescence kinetics of A_1 and the former ($D \rightarrow A_1$) as a positive component.

4.1. FDAS of G. violaceus

For simulation of FDAS, common lifetimes were adopted for intact cells, PBSs, and rod assemblies, and the results are shown in Fig. 7. To analyze the TRFS of intact cells, five components were necessary (SVD analysis): shorter than 10 ps (hereafter referred to as the 10-ps component), 35 ps, 95 ps, 420 ps, and longer than 1 ns (hereafter referred to as the long-lived component). For rod assemblies and PBSs, the shortest lifetime component was not resolved, but four components were sufficient (35-ps, 95-ps, 420-ps, and a long-lived component). Hereafter, FDAS were analyzed more in detail in individual samples.

4.1.1. FDAS of G. violaceus intact cells

The 10-ps component was resolved only in intact cells. A negative peak at 572 nm mainly contributed to this component. There was no positive signal in any lifetime component in the wavelength region shorter than 572 nm, therefore there may be an unresolved energy donor transferred to PE_{572} with a time constant faster than our time resolution. Phycourobilin in PE was most probably the energy donor to PE_{572} as shown by the steady-state absorption spectrum (Fig. 2a). Negative peaks were recognized also in the PC region. However, because of arrangement of chromophores and discs, these could not be assigned to energy transfers from phycourobilin. As discussed later, the negative peaks in PC region were also detected in green light grown *F. diplosiphon* that contained only phycoerythrobilin in PE. Therefore, it is likely that the negative peak mainly comes from fast energy transfer in PC. Coupling of a negative 640-nm band in the 10-ps and 35-ps components and a positive 640-nm band in the 95-ps and 420-ps components

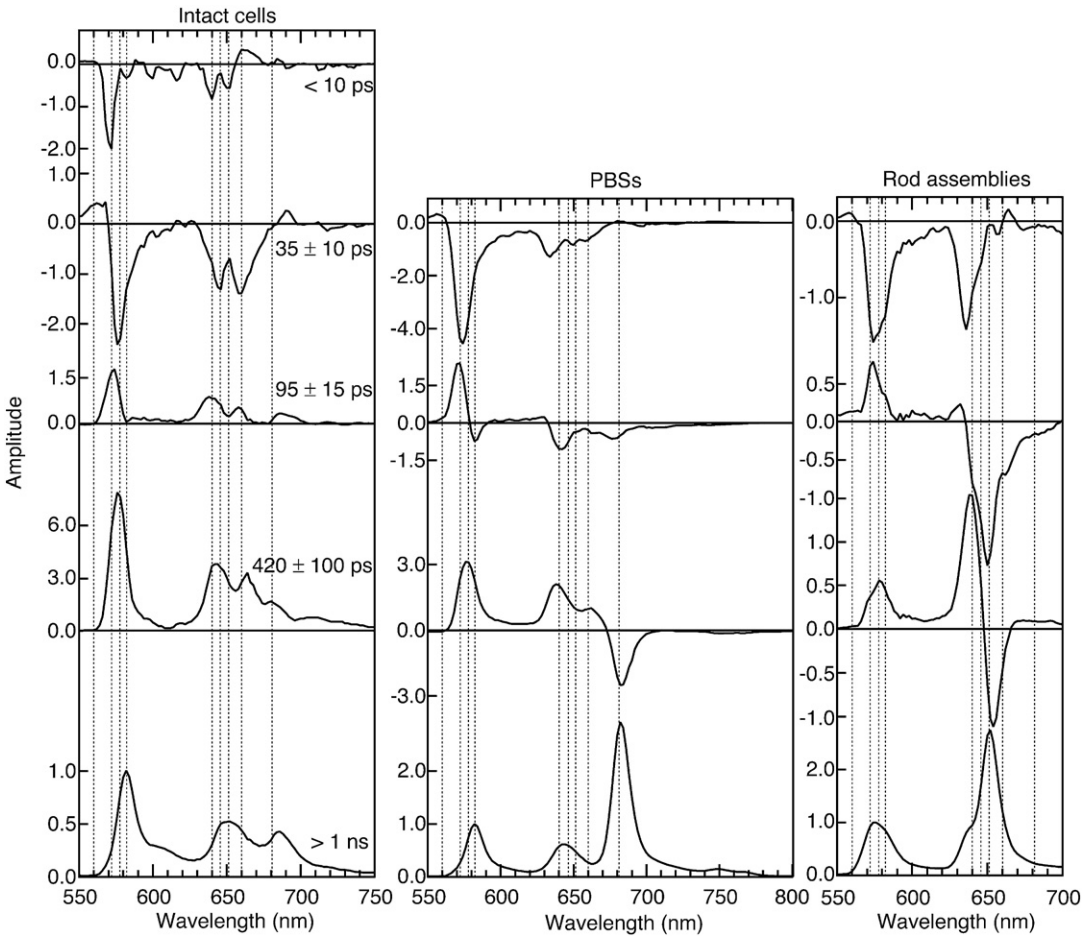

Fig. 7. FDAS of intact cells, PBSs, and rod assemblies of *G. violaceus*. FDAS were resolved on the basis of TRFS shown in Fig. 5. Note that FDAS amplitudes were normalized at PE wavelength region. Vertical dashed lines indicate locations of typical bands at 560, 572, 578, 582, 640, 646, 651, 660, and 680 nm.

indicates the slower PE→PC energy transfer (≈95 ps and ≈420 ps), followed by a subsequent faster energy transfer (<10 ps and 35 ps) in PC. The existence of positive peaks in the PE region in the 95-ps and 420-ps components confirmed this slower PE→PC energy transfer.

A fast energy transfer pathway from PE_{560} (a positive peak) to PE_{578} (a negative peak) in PE was recognized in the 35-ps component, however PE_{572} was not involved in this pathway. APC_{660} exhibited a negative peak in the 35-ps component, indicating a fast energy transfer from PC to APC_{660}, which is consistent with the previous result [23]. A positive peak at 690 nm in the 35-ps component came from PS I Chl *a* [33]. A positive peak around 685 nm came from PS II Chl *a* [22,34]. PS I Chl *a* showed a small amplitude in the 95-ps component around 680–690 nm [33], however it was no longer observed in components with a longer lifetime. The 420-ps component showed a positive peak at 578 nm, indicating PE_{578} also transfers energy to PC with this time constant. A peak around 682 nm originated from both the APC terminal emitter(s) and PS II Chl *a* [22,34].

Time constants of the long-lived component varied in wavelength, indicating decay of individual fluorescence components. In the PE region, a positive peak at 582 nm with a broad band around 608 nm decayed with a time constant of 2.5 ns, which is identical to the lifetime of isolated PE hexamer [20]. On the other hand, in the PC–APC region, positive peaks around 650 nm and 660 nm with a shoulder around 640 nm decayed with a 1.8-ns lifetime, which is identical to the lifetime of isolated PC and APC [20]. These data indicate that the long-lived component mainly reflects fluorescence from the chromophores that did not virtually transfer energy to other chromospheres. A positive peak at 684 nm, which decayed with a 2.1-ns lifetime, came from PS II Chl *a* [34,35]. The amplitudes of long-lived components were lower than 10%, indicating that an over-all energy transfer efficiency from phycobiliproteins to Chl *a* is not necessarily high.

4.1.2. FDAS of G. violaceus PBSs

In PBSs, the whole fluorescence decay curves were simulated by four components; the 10-ps lifetime component was not resolved. The 35-ps component was similar to that of intact cells except for a slight blue-shift of the negative peaks. In intact cells, the fast energy transfers occurred at PE_{572} and PC_{640} (<10 ps).

The 95-ps component of PBSs in the PE region showed peaks at almost the same wavelengths as that of intact cells, showing energy transfer from PE_{572}. In the PC region, the 95-ps component of PBSs showed negative peaks, whereas that of

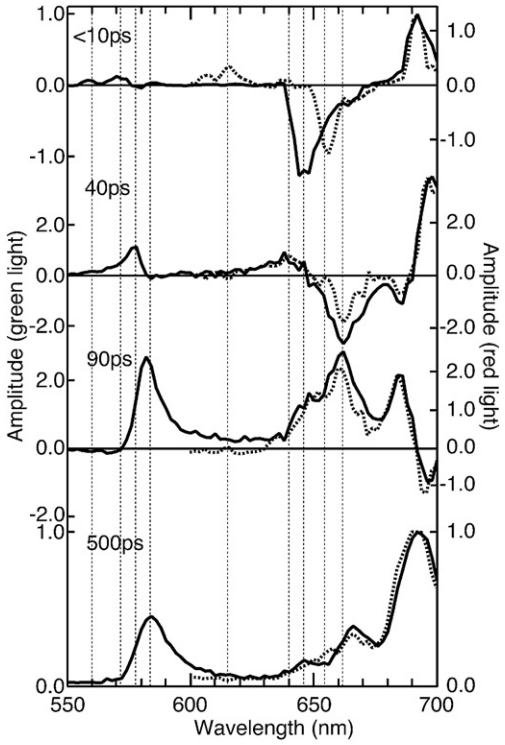

Fig. 8. FDAS of *F. diplosiphon* growth under green light (solid line, left axis) and red light (dashed line, right axis). FDAS were resolved on the basis of TRFS shown in Fig. 6. Each spectrum was normalized at Chl *a* wavelength region. Vertical dashed lines indicate locations of typical bands at 560, 572, 578, 584, 615, 640, 646, 654, and 662 nm.

intact cells showed positive peaks. This is because the contribution of the fast energy transfer (< 10 ps) in PC was negligibly small in PBSs. A negative peak at 682 nm in the 95-ps component was assigned to a fast phase of an energy transfer to APC_{682}. In the APC region of the 420-ps component, a positive peak around 660 nm and a negative peak at 682 nm was observed, indicating a slow energy transfer from APC_{660} to APC_{682}.

The long-lived component of PBS was almost the same as that of intact cells except for behaviors of the red-most fluorescence in each fluorescence region; (i) in the PE region, a broad band around 608 nm, which was specifically found in intact cells, decreased in relative intensity against the 582-nm band, (ii) in the PC region, the 650-nm band decreased in relative intensity against the peak around 640 nm, and (iii) in the APC region, a positive peak was observed at 682 nm, which came from the APC terminal emitter (APC_{682}) (APC-B and/or L_{CM}) with vibrational bands at 750 nm and 768 nm (Fig. 3b).

4.1.3. FDAS of G. violaceus rod assemblies

In rod assemblies, the whole fluorescence decay curves were simulated by four components, as is the case for PBSs; the 10-ps lifetime component was not necessary for the best fit. The four components showed similar spectra to those observed in PBSs, but two distinctive features were recognized. Firstly, the 582-nm band was clearly resolved in all the lifetime components; however, the 572-nm band became dominant in the long-lived components. This suggests that some routes of the $PE_{572} \rightarrow PE_{582}$ energy transfer pathway (95 ps) were lost in rod assemblies. The slow energy transfer pathway (95 ps) from the PE_{582} was conserved in rod assemblies. Secondly, PC_{651} showed negative peaks in the 95-ps and 420-ps components and a positive peak in the long-lived component, which reflects that PC_{651} works as an energy reservoir due to the lack of PC → APC energy transfer in rod assemblies. A characteristic decay process in rod assemblies was the slow energy transfer among the pigments that transfers energy to the terminal form of PC. The 420-ps components of intact cells and PBSs showed the positive peak at 640 nm with a valley around 654 nm, indicating the conservation of the slow energy transfer in intact cells and PBSs.

4.1.4. Energy transfer in G. violaceus

Based on the analysis of FDAS, we concluded the following energy transfer pathways (Fig. 9). Phycourobilin probably transferred energy to PE_{572} (the 10-ps component). PE_{582}

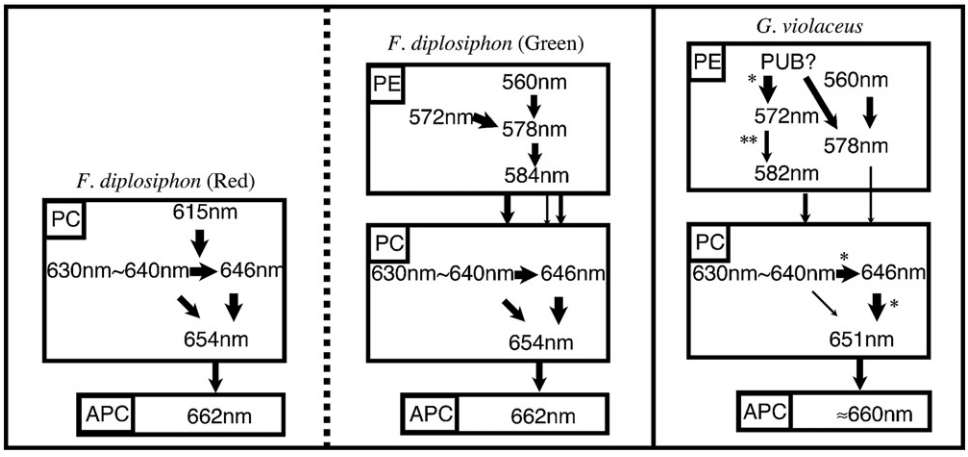

Fig. 9. Schematic model for energy transfer pathways in PBSs of *G. violaceus* and *F. diplosiphon* grown under two light conditions. Models were shown on the basis of FDAS measured at −196 °C. Four types of arrows indicate differences in the energy transfer rate; thicker arrows indicate faster energy transfer time constants that were resolved by FDAS analysis. Asterisks and a double asterisk indicate the pathways that occurred with longer time constants both in isolated PBSs and rod assemblies and only in rod assemblies, respectively.

accepted energy from PE_{572}, and subsequently transferred energy to PC slowly (the 95-ps components). PE_{578} also accepted energy from PE_{560} (the 35-ps components), and subsequently transferred energy to PC more slowly (the 420-ps components). We concluded the presence of multiple energy donors to PC, i.e., PE_{578} and PE_{582}. PC_{640} accepted energy from PE slowly (the 95-ps and 420-ps components) and transferred energy quickly toward PC_{651} (the 10-ps component). The large energy migration process before energy transfer to PC_{651} may result from the slow energy transfer pathway (the 420-ps components). APC_{660} accepted energy from PC (the 35-ps components), and transferred energy to APC_{682} (the 95-ps and 420-ps components).

4.2. FDAS of F. diplosiphon

Fig. 8 shows FDAS of *F. diplosiphon*. We analyzed the decay curves exclusively in the wavelength region up to PS II Chl *a* (700 nm), because fluorescence intensities in the PS I Chl *a* region were so high that they hindered the analysis of the remaining low intensity region. Four components, i.e. a short-lived component (<10 ps), 40-ps, 90-ps, and 500-ps components, were necessary to fit to the whole decay processes. Amplitudes of the lifetime component longer than 1 ns were lower than 5% in the wavelength region shown in Fig. 8 (550–700 nm); therefore, those were not included in the analyses. Even by this treatment in the global analysis, the essential results remained identical to those obtained after calculation of the whole wavelength region. The numbers of peak positions based on steady-state fluorescence measurements were smaller than those based on FDAS, which indicates efficient energy transfer in *F. diplosiphon*. The peaks that appeared in both measurements mainly reflect the terminal energy donors in each of the biliproteins.

4.2.1. FDAS of F. diplosiphon grown under green light

Chromophores of PE in *F. diplosiphon* are phycoerythrobilins. In the short-lived component, the positive peak around 572 nm showed similar intensity to the negative peak around 578 nm (Fig. 8, full lines), which was different from *G. violaceus* (Fig. 7). This may be related to absence of phycourobilin in *F. diplosiphon*. The short-lived component showed a negative peak around 646 nm with shoulders around 656 nm and 666 nm. Since PE_{584} of *F. diplosiphon* has 40-ps, 90-ps, and 500-ps components that are responsible for energy transfers to PC, the negative peaks around 646 nm mainly reflected slow energy transfer from PE to PC_{646} and a subsequent fast energy transfer (<10 ps). In the PC–APC region, the 40-ps component showed a positive peak around 640 nm and a negative peak at 662 nm with a negative shoulder around 654 nm, which reflects energy transfer from PC_{640} to APC_{662} via PC_{654}. The positive peak around 640 nm showed smaller integrated intensity than the negative peak around 662 nm. The positive amplitude (energy transfer to APC_{662}) and the negative amplitude (energy transfer from PE_{584}) may have cancelled each other at around 640 nm [36]. Reflecting slow energy transfer from PE_{584} to PC, the 90-ps and 500-ps components showed peaks at 584 nm and around 650 nm. The positive peak at 660 nm in the 90-ps and 500-ps components may reflect a slow energy transfer from APC_{660}. The 500-ps component showed positive peaks at 584 nm, 650 nm, and 666 nm that came from PE, PC, and APC, respectively.

In the wavelength region longer than 680 nm, the fluorescence kinetics included energy transfer processes among the PS II Chl *a* and those among the PS I Chl *a* [33,34]. The 690-nm and 696-nm bands in the short-lived and 40-ps components were assigned to the short-wavelength forms of the PS I Chl *a*, whereas the 685-nm band in the 40-ps component and the bands in 680–700 nm in the 90-ps and 500-ps components were assigned to the PS II Chl *a*.

4.2.2. FDAS of F. diplosiphon grown under red light

Four components were necessary to fit to the whole decay processes (Fig. 8, dashed lines); their time constants were set to be identical to those found for the FDAS of the green-grown cells. The short-lived components showed spectral features depending on the light conditions for growth. In the red-grown cells of *F. diplosiphon*, the main peak with a negative amplitude was found at 654 nm, which was red-shifted by 9 nm compared with the green-grown cells, probably reflecting successive fast energy transfer in PC and APC. In addition, a positive peak around 615 nm was observed, which came from the PC form (PC_{615}) induced under red light. Except for relative intensities against the Chl *a* band, the FDAS of the 40-ps, 90-ps, and 500-ps components of *F. diplosiphon* grown under red light were similar to those of the green-grown cells; this indicated that energy transfer processes remained identical, irrespective of difference in the pigment composition of PBS rods.

4.2.3. Energy transfer in F. diplosiphon

Based on the analysis of FDAS, we concluded the following energy transfer pathways (Fig. 9): PE_{572} transferred energy to PE_{578} (the short-lived component). PE_{584} accepted energy from PE_{578}, and transferred energy to PC (the 40-ps, 90-ps, and 500-ps components). The energy donor to PC was only PE_{584}, and a subsequent fast energy transfer occurred in PC (the short-lived component). The red-grown cells showed PC_{615} additionally, which transferred energy quickly to PC (the short-lived component). APC_{660} accepted energy from PC (the 40-ps component), and transferred its energy slowly (the 90-ps component).

5. Discussion

Energy transfer processes of PBSs have been analyzed by time-resolved fluorescence spectroscopy because fluorescence peaks directly correspond to energy levels of pigments and energy transfer is expressed as dynamic peak shifts or dynamic peak alterations. A combination of the fluorescence decay curves and global analysis yielded FDAS as similar to absorption changes. Time resolution has improved during the last 20 years, however spectral resolution has not necessarily been fully improved. Our current analysis was conducted with a spectral resolution of 2 nm and time resolution of 3 ps, however

we cannot resolve the fastest energy transfer process between two specific chromophores in APC that is known to occur in a time range of 500 fs [37]. In addition, an intermediate that plays a role of acceptor and donor at the same time with similar efficiency cannot be detected by spectral analysis. Even under these analytical conditions, we could resolve many spectral forms that were shown by the second derivative spectra of the steady-state spectrum and described their time behavior in this study.

In hemidiscoidal PBS of *F. diplosiphon*, PE_{584} transferred energy to PC (the 40-ps, 90-ps, and 500-ps components). These values were similar to previously reported time constants of 60 ps, 91 ps, and 728 ps [38], even though differences in the fluorescence maxima among the three were not mentioned. The PC→APC energy transfer kinetics observed in the 40-ps components was also consistent with the previous result [23]. These are energy transfers between different types of phycobiliproteins, such as PE to PC, or PC to APC. Energy transfer in isolated PC and APC trimers has been studied previously [37,39]. Intact cells and isolated PBSs of various cyanobacteria were also measured by time-resolved spectroscopy [40–42]. Recently, transfer constants between two PC hexamers were calculated using a semi-empirical approach, where the fastest time constant is 13.7 ps [43]. However, the kinetics of energy transfer between PE and PE, or PC and PC in PBSs rod structure has not been measured well [12]. We analyzed kinetics more in detail within PE and PC using the FDAS of intact cells, isolated PBSs, and rod assemblies. Improved spectral resolution was needed to reveal energy transfer kinetics between the same types of phycobiliproteins. Critical points for analysis were the presence of phycourobilin in PE of *G. violaceus* and energy migration among rod assemblies in PBSs. As for *F. diplosiphon*, differences in the pigment composition may induce new spectral form(s) in PC, and this may link to the differentiation of PC forms in PBSs.

Schematic models for energy transfer processes in the three samples are schematically shown in Fig. 9 with spectral forms and qualitative transfer times used for FDAS. In *G. violaceus*, the very fast processes were observed in the transfer pathways of phycourobilin→PE_{572} and PC_{646}→PC_{651}. The transfers from phycourobilin and PE_{560} to PE_{578} were also fast. However, the PE→PC transfer was slow, even though two pathways were resolved. On the contrary, energy transfer in the PE of *F. diplosiphon* grown under green light was fast even though four spectral forms were resolved. Furthermore, the PE→PC transfer was also fast. This may reflect the difference of linker protein [16] and/or the large energy migration before energy transfer to PC. The hemiellipsoidal PBS isolated from *Porphyridium cruentum*, the rods of which also contain PE and PC [44,45], showed both fast and slow PE → PC energy transfers, subsequently to APC [40]. Therefore, we concluded that the lack of fast pathway in the PE→PC energy transfer in *G. violaceus* results from a different linker protein. *F. diplosiphon* grown under red light contains an additional PC form and this was involved in the fast transfer pathway. The PC→APC energy transfer showed similar kinetics in the three cases. APC_{660} transferred energy to APC_{680} slowly (the 95-ps and 420-ps components of *G. violaceus* PBSs). These time constants seemed slower than the constant of 55 ps observed in the isolated APC-B trimer [24]. APC-B trimers formed the APC core complex with APC trimers. A previous report showed 45-ps and 110-ps time constants for the energy migration in the APC trimer [23]. Large energy migration within the APC core complex may relate to the slow energy transfer from APC_{660} to APC_{680}.

PC_{615} was specific in the red-grown cells of *F. diplosiphon*, and the energy transfer from this form was very fast. The red-grown cells contained two additional PC hexamers that are induced under red light illumination (Fig. 1) [25]. Under green light, these PC hexamers in *F. diplosiphon* were replaced with PE hexamers. On the other hand, *G. violaceus* was considered to contain three PC hexamers and three PE hexamers simultaneously. The short-lived component of *F. diplosiphon* grown under green light showed no signal at 615 nm, whereas that of *G. violaceus* showed a small negative signal (Figs. 7 and 8). This suggests that most of PC_{615} does not attach directly to APC. The energy transfer from PE may make the signal at 615 nm indistinct in *G. violaceus*. The negative peak around 646 nm showed lower intensity in *F. diplosiphon* grown under red light, whereas that grown under green light showed peak maxima around 646 nm. The time-dependent behaviors of other lifetime components were very similar to those of the green-grown cells, indicating the preserved energy transfer processes.

The bundle-like PBSs of *G. violaceus* showed slow kinetics that may be caused by energy migration in rod assemblies. The existence of slow pathways (95-ps and 420-ps components) does not seem an appropriate property, however the S_1 lifetime of isolated phycobiliprotein is known to be much longer [24], thus an over-all efficiency of energy transfer remains significant. On the other hand, the bundle-like PBSs contain larger amounts of biliprotein than the hemidiscoidal PBSs in the same basal area. This is an advantage when *G. violaceus* harvests light energy under low light conditions with its small surface area of cell membranes. *G. violaceus* grows only under low light conditions, therefore the bundle-like PBSs seem suitable for *G. violaceus* growth.

We analyzed the energy transfer kinetics in the bundle-like PBSs of *G. violaceus* and hemidiscoidal PBSs of *F. diplosiphon* using global analysis of fluorescence decay curves with improved spectral resolution (Fig. 9). The observed differences in these two types of PBS are summarized as follows: (1) The bundle-like PBSs of *G. violaceus* showed only slow energy transfer pathways from the PE_{578} and PE_{582} to PC, which may relate to a novel linker protein. The fast energy transfer from PE_{578} to PE_{582} was not observed. (2) The presence of phycourobilin in PE of *G. violaceus* contributes to the fast energy transfer pathways to PE_{572} and PE_{578}. The fast energy transfer pathway from PE_{560} to PE_{578} was conserved between two types of PBSs. (3) The energy migration processes in the bundle-like PBSs slow down the effective energy transfer rates to the terminal emitters (PE_{582} and PC_{651}). The fast pathway from PC to APC via PC_{646} and PC_{651} was similar between two types of PBSs. (4) In the hemidiscoidal PBSs of *F. diplosiphon*, the PC form induced under red light related to the fast energy

transfer to the other forms of PC, which was not the case in the bundle type. The methods adopted in this study were useful for analyzing antenna systems consisting of multiple components.

Acknowledgements

We thank Prof. Emer. I. Yamazaki, Hokkaido University, for his help with the TRFS measurements. This study was supported in part by a Grant-in-Aid for Creative Scientific Research (No.17GS0314) from the Japanese Society for the Promotion of Science and by Scientific Research on Priority Areas "Comparative Genomics" (Nos. 17018022 and 18017016) from the Ministry of Education, Sports, Culture, Science, and Technology, Japan, to MM, and by a Grant-in-Aid for Scientific Research (No. 18350067) to SA.

References

[1] E. Mörschel, K.P. Koller, W. Wehrmeyer, H. Schneider, Biliprotein assembly in the disc-shaped phycobilisomes of *Rhodella violacea* I. Electron microscopy of phycobilisomes in situ and analysis of their architecture after isolation and negative staining, Cytobiologie 16 (1977) 118–129.

[2] E. Mörschel, The light-harvesting antennae of cyanobacteria and red algae, Photosynthetica 25 (1991) 137–144.

[3] A.N. Glazer, Adaptive variations in phycobilisome structure, Adv. Mol. Cell Biol. 10 (1994) 119–149.

[4] W.A. Sidler, Phycobilisome and phycobiliprotein structures, in: D.A. Bryant (Ed.), The molecular biology of cyanobacteria, Kluwer Academic Publishers, Dordrecht, 1994, pp. 139–216.

[5] W. Reuter, G. Wiegand, R. Huber, M.E. Than, Structural analysis at 2.2 Å of orthorhombic crystals presents the asymmetry of the allophycocyanin-linker complex, AP.$L_C^{7.8}$, from phycobilisomes of *Mastigocladus laminosus*, Proc. Natl. Acad. Sci. U. S. A. 96 (1999) 1363–1368.

[6] C. Contreras-Martel, J. Martinez-Oyanedel, M. Bunster, P. Legrand, C. Piras, X. Vernede, J.C. Fontecilla-Camps, Crystallization and 2.2 Å resolution structure of R-phycoerythrin from *Gracilaria chilensis*: a case of perfect hemihedral twinning, Acta Crystallogr. D57 (2001) 52–60.

[7] E. Gantt, B. Grabowski, F.X. Cunningham Jr., Antenna systems of red algae: phycobilisomes with photosystem II and chlorophyll complexes with photosystem I, in: B.R. Green, W.W. Parson (Eds.), Light-harvesting antennas in photosynthesis, Kluwer Academic Publishers, Dordrecht, 2003, pp. 307–322.

[8] M. Mimuro, H. Kikuchi, Antenna systems and energy transfer in Cyanophyta and Rhodophyta, in: B.R. Green, W.W. Parson (Eds.), Light-Harvesting Antennas in Photosynthesis, Kluwer Academic Publishers, Dordrecht, 2003, pp. 281–306.

[9] A.R. Holzwarth, Light absorption and harvesting, in: M.D. Archer, J. Barber (Eds.), Molecular to global photosynthesis, Imperial College Press, London, 2004, pp. 43–115.

[10] M. Mimuro, Photon capture, exciton migration and trapping and fluorescence emission in cyanobacteria and red algae, in: G.C. Papageorgiou, Govindjee (Eds.), Chlorophyll Fluorescence: The signature of plant productivity, Kluwer Academic Publishers, Dordrecht, 2004, pp. 173–195.

[11] L.-N. Liu, X.-L. Chen, Y.-Z. Zhang, B.-C. Zhou, Characterization, structure and function of linker polypeptides in phycobilisomes of cyanobacteria and red algae: an overview, Biochim. Biophys. Acta 1708 (2005) 133–142.

[12] J. Zhao, H. Li, The excitation energy transfer in photosynthesis of cyanobacteria, in: N. Wada, M. Mimuro (Eds.), Recent progress of bio/chemiluminescence and fluorescence analysis in photosynthesis, Research Signpost, Kerala, 2005, pp. 175–192.

[13] J. Nield, P.J. Rizkallah, J. Barber, N.E. Chayen, The 1.45 Å three-dimensional structure of C-phycocyanin from the thermophilic cyanobacterium *Synechococcus elongatus*, J. Struct. Biol. 141 (2003) 149–155.

[14] R. Rippka, J. Waterbury, G. Cohen-Bazire, A cyanobacterium which lacks thylakoids, Arch. Microbiol. 100 (1974) 419–436.

[15] G. Guglielmi, G. Cohen-Bazire, D.A. Bryant, The structure of *Gloeobacter violaceus* and its phycobilisomes, Arch. Microbiol. 129 (1981) 181–189.

[16] K. Koyama, T. Tsuchiya, S. Akimoto, M. Yokono, H. Miyashita, M. Mimuro, New linker proteins in phycobilisomes isolated from the cyanobacterium *Gloeobacter violaceus* PCC 7421, FEBS Lett. 580 (2006) 3457–3461.

[17] E. Selstam, D. Campbell, Membrane lipid composition of the unusual cyanobacterium *Gloeobacter violaceus* sp. PCC 7421, which lacks sulfoquinovosyl diacylglycerol, Arch. Microbiol. 166 (1996) 132–135.

[18] Y. Nakamura, T. Kaneko, S. Sato, M. Mimuro, H. Miyashita, T. Tsuchiya, S. Sasamoto, A. Watanabe, K. Kawashima, Y. Kishida, C. Kiyokawa, M. Kohara, M. Matsumoto, A. Matsuno, N. Nakazaki, S. Shimpo, C. Takeuchi, M. Yamada, S. Tabata, Complete genome structure of *Gloeobacter violaceus* PCC 7421, a cyanobacterium that lacks thylakoids, DNA Res. 10 (2003) 137–145.

[19] E.B. Gutiérrez-Cirlos, B. Pérez-Gómez, D.W. Krogmann, C. Gómez-Lojero, The phycocyanin-associated rod linker proteins of the phycobilisome of *Gloeobacter violaceus* PCC 7421 contain unusually located rod-capping domains, Biochim. Biophys. Acta 1757 (2006) 130–134.

[20] I. Yamazaki, M. Mimuro, T. Murao, T. Yamazaki, K. Yoshihara, Y. Fujita, Excitation energy transfer in the light harvesting antenna system of the red alga *Porphyridium cruentum* and the blue-green alga *Anacystis nidulans*: analysis of time-resolved fluorescence spectra, Photochem. Photobiol. 39 (1984) 233–240.

[21] M. Mimuro, I. Yamazaki, T. Yamazaki, Y. Fujita, Excitation energy transfer in the chromatically adapted phycobilin systems of blue-green algae: difference in the energy transfer kinetics at phycocyanin level, Photochem. Photobiol. 41 (1985) 597–603.

[22] E. Bittersmann, W. Vermaas, Fluorescence lifetime studies of cyanobacterial photosystem II mutants, Biochim. Biophys. Acta 1098 (1991) 105–116.

[23] J.-m. Zhang, J.-q. Zhao, L.-j. Jiang, X.-g. Zheng, F.-l. Zhao, H.-z. Wang, Studies on the energy transfer among the rod-core complex from phycobilisome of *Anabaena variabilis* by time resolved fluorescence emission and anisotropy spectra, Biochim. Biophys. Acta 1320 (1997) 285–296.

[24] T. Yamazaki, Y. Nishimura, I. Yamazaki, M. Hirano, K. Matsuura, K. Shimada, M. Mimuro, Energy migration in allophycocyanin-B trimer with a linker polypeptide: analysis by the principal multi-component spectral estimation (PMSE) method, FEBS Lett. 353 (1994) 43–47.

[25] E.L. Stowe-Evans, D.M. Kehoe, Signal transduction during light-quality acclimation in cyanobacteria: a model system for understanding phytochrome-response pathways in prokaryotes, Photochem. Photobiol. Sci. 3 (2004) 495–502.

[26] A. Savitzky, M.J.E. Golay, Smoothing and differentiation of data by simplified least squares procedures, Anal. Chem. 36 (1964) 1627–1639.

[27] S. Akimoto, M. Yokono, M. Ohmae, I. Yamazaki, A. Tanaka, M. Higuchi, T. Tsuchiya, H. Miyashita, M. Mimuro, Ultrafast excitation relaxation dynamics of lutein in solution and in the light-harvesting complexes II Isolated from *Arabidopsis thaliana*, J. Phys. Chem. B 109 (2005) 12612–12619.

[28] A.R. Holzwarth, Data analysis of time-resolved measurements, in: J. Amesz, A.J. Hoff (Eds.), Biophysical techniques in photosynthesis, Kluwer Academic Publishers, Dordrecht, 2004, pp. 75–92.

[29] D. Mangels, J. Kruip, S. Berry, M. Rögner, E.J. Boekema, F. Koenig, Photosystem I from the unusual cyanobacterium *Gloeobacter violaceus*, Photosynth. Res. 72 (2002) 307–319.

[30] M. Mimuro, T. Ookubo, D. Takahashi, T. Sakawa, S. Akimoto, I. Yamazaki, H. Miyashita, Unique fluorescence properties of a cyanobacterium *Gloeobacter violaceus* PCC 7421: reasons for absence of the long-wavelength PSI Chl *a* fluorescence at −196 °C, Plant Cell Physiol. 43 (2002) 587–594.

[31] M. Mimuro, C. Lipschultz, E. Gantt, Energy flow in the phycobilisome core of *Nostoc* sp. (MAC): two independent terminal pigments, Biochim. Biophys. Acta 852 (1986) 126–132.

[32] B. Szalontai, Z. Gombos, V. Csizmadia, K. Csatorday, M. Lutz, Chromophore states in allophycocyanin and phycocyanin. A resonance Raman study, Biochemistry 28 (1989) 6467–6472.

[33] L.-O. Palsson, S.E. Tjus, B. Andersson, T. Gillbro, Energy transfer in photosystem I. Time resolved fluorescence of the native photosystem I complex and its core complex, Chem. Phys. 194 (1995) 291–302.

[34] M. Komura, Y. Shibata, S. Itoh, A new fluorescence band F689 in photosystem II revealed by picosecond analysis at 4–77 K: Function of two terminal energy sinks F689 and F695 in PS II, Biochim. Biophys. Acta 1757 (2006) 1657–1668.
[35] M. Mimuro, S. Akimoto, T. Tomo, M. Yokono, H. Miyashita, T. Tsuchiya, Delayed fluorescence observed in the nanosecond time region at 77 K originates directly from the photosystem II reaction center, Biochim. Biophys. Acta 1767 (2007) 327–334.
[36] C.D. van der Weij-de Wit, J.A. Ihalainen, R. van Grondelle, J.P. Dekker, Excitation energy transfer in native and unstacked thylakoid membranes studied by low temperature and ultrafast fluorescence spectroscopy, Photosynth. Res. (in press).
[37] T. Gillbro, A.V. Sharkov, I.V. Kryukov, E.V. Khoroshilov, P.G. Kryukov, R. Fischer, H. Scheer, Foerster energy transfer between neighboring chromophores in C-phycocyanin trimers, Biochim. Biophys. Acta 1140 (1993) 321–326.
[38] D. Frackowiak, A. Kowalczyk, A. Skibinski, Analysis of time-resolved emission spectra of oriented phycobilisomes, Biophys. Chem. 42 (1992) 153–161.
[39] A.V. Sharkov, I.V. Kryukov, E.V. Khoroshilov, P.G. Kryukov, R. Fischer, H. Scheer, T. Gillbro, Femtosecond energy transfer between chromophores in allophycocyanin trimers, Chem. Phys. Lett. 191 (1992) 633–638.
[40] J. Wendler, A.R. Holzwarth, W. Wehrmeyer, Picosecond time-resolved energy transfer in phycobilisomes isolated from the red alga *Porphyridium cruentum*, Biochim. Biophys. Acta 765 (1984) 58–67.
[41] M. Mimuro, I. Yamazaki, N. Tamai, T. Katoh, Excitation energy transfer in phycobilisomes at −196 °C isolated from the cyanobacterium *Anabaena variabilis* (M-3): evidence for the plural transfer pathways to the terminal emitters, Biochim. Biophys. Acta 973 (1989) 153–162.
[42] C.W. Mullineaux, E. Bittersmann, J.F. Allen, A.R. Holzwarth, Picosecond time-resolved fluorescence emission spectra indicate decreased energy transfer from the phycobilisome to photosystem II in light-state 2 in the cyanobacterium *Synechococcus* 6301, Biochim. Biophys. Acta 1015 (1990) 231–242.
[43] A.R. Matamala, D.E. Almonacid, M.F. Figueroa, J. Martinez-Oyanedel, M.C. Bunster, A semiempirical approach to the intra-phycocyanin and inter-phycocyanin fluorescence resonance energy-transfer pathways in phycobilisomes, J. Comp. Chem. 28 (2007) 1200–1207.
[44] A.N. Glazer, C.S. Hixson, Subunit structure and chromophore composition of rhodophytan phycoerythrins. *Porphyridium cruentum* B-phycoerythrin and b-phycoerythrin, J. Biol. Chem. 252 (1977) 32–42.
[45] M. Westermann, W. Wehrmeyer, A new type of complementary chromatic adaptation exemplified by *Phormidium* sp. C86: changes in the number of peripheral rods and in the stoichiometry of core complexes in phycobilisomes, Arch. Microbiol. 164 (1995) 132–141.